ISBN: 978-3-95450-214-1 ISSN: 2673-5490 doi:10.18429/JACoW-IPAC2021-FRXB07

INJECTOR OPTIMIZATION FOR THE IR-FEL OPERATION AT THE COMPACT ERL AT KEK*

O. A. Tanaka†, T. Miyajima, N. Higashi
High Energy Accelerator Research Organization, KEK, Tsukuba, Japan

Abstract

The Compact Energy Recovery Linac (cERL) at KEK is a test accelerator to develop ERL technologies and to operate with a high average beam current and a high beam quality. cERL consists of a photoinjector, a main linac (ML) for energy recovery, a recirculation loop and a beam dump (see Fig. 1). A recent upgrade of the cERL to the middle Infrared Free Electron Laser (IR-FEL) imposed new conditions to maintain beam parameters. Therefore, the injector should be optimized to meet the following requirements at the exit of the main linac. The rms bunch length should be 2 ps, the rms longitudinal emittance should be kept the least, and simultaneously the rms transverse emittance should be kept less than 3 π mm mrad. In this work we describe the strategy and results of the injector optimization to achieve the better performance of the cERL-FEL.

INTRODUCTION

The Compact Energy Recovery Linac at KEK was originally built as a test accelerator to develop ERL technologies and to operate with a high average beam current and a high beam quality [1]. Since project restart in 2017 a high charge pulse mode operation to develop a beam handling method towards high average current FEL was done in March 2017 [2] and March 2018 [3]. Then in June 2018 we succeed in CW operation with the average current of 1 mA and with energy recovery [4]. This operation lasted for 2 hours, and was allowed by the stable performance of the 500 kV photocathode DC gun [5].

In 2019 the cERL IR-FEL project has been launched. This project aimed at developing high-power middle infrared lasers for high-efficiency laser processing [6]. After the 1st undulator was installed into the beam line in March 2020, we have started FEL tests with the development of the tuning procedure. The construction of the cERL IR-FEL was completed in May 2020 in spite of COVID-19 [7]. FEL tests were continued in June, when the 2nd undulator has been already installed [8]. Last commissioning was performed in February and March 2021. We have developed a tuning procedure for the FEL light production. As a result of cERL IR-FEL project we had realized the first ERL-based single-pass FEL in the world (for more details refer to Kato at [9]).

This work is concentrated on the injector optimization for successful production of the IR-FEL light. A typical injector optimization aims to achieve a peak performance in the injector. However, we need to generate and to transport appropriate beam to the undulator entrance (see Point U at Fig. 1). Accordingly, particular requirements to maintain beam parameters (listed below) are imposed at the point where the injector part is matched into the resirculation loop. In our case this point (see Point A2 at Fig. 1) is at the exit of the ML. This matching point was chosen to facilitate the optics matching procedure.

Thus, details and results of the injector optimization are described in the next section. A comparison of the designed injector performance with measured results and its discussion are given in the rest part of the manuscript.

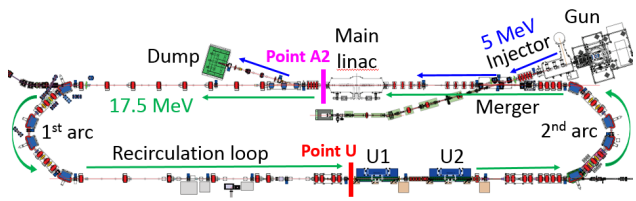

Figure 1: Layout of the cERL.

INJECTOR OPTIMIZATION

As it was mentioned in the Introduction, a suitable beam should be delivered to the exit of an undulator in order to produce the FEL light. Requirements to the beam performance at the undulator entrance read: the bunch charge of 60 pC and the repetition rate of 1.3 GHz, the bunch length: 0.5 – 2 ps, the energy spread of 0.1%, and the normalized rms transverse emittance of about 3 π mm mrad. Accordingly, the target beam performance at the ML exit includes the bunch charge of 60 pC, the bunch length of 2 ps (rms), the energy spread of 0.1%, and the normalized rms transverse emittance less than 3 π mm mrad.

Influence of the Electron Gun Voltage

The beam performance is assured by the stable and high accelerating voltage supply of the DC gun. Unfortunately, in November last year we had a trouble during gun processing. Due to this misoperation, the voltage of the photocathode DC gun dropped. The final conditioning gave 480 kV of accelerating voltage instead of typical 500 kV. So, the question arose: can the necessary beam performance still be achieved? To address this question we had been studying how the DC gun accelerating voltage effects on the beam performance.

Injector optimization was done in General Particle Tracer (GPT, [10]) with Multi Objective Genetic Algorithm (MOGA, [11]). The objectives of this optimization was set

* Work supported by the NEDO project "Development of next generation laser technology with high brightness and high efficiency".
† olga@post.kek.jp

ISBN: 978-3-95450-214-1 ISSN: 2673-5490 doi:10.18429/JACoW-IPAC2021-FRXB07

up to simultaneously minimize the bunch length and transverse emittance at the exit of the ML (Fig. 1). Thus, the gun voltage was scanned from 500 kV to 375 kV with the 25 kV step. Figure 2 demonstrates the optimization results for the rms bunch length vs transverse (Fig. 2 (a)) and the rms bunch length vs longitudinal (Fig. 2 (b)) emittances at the exit of ML. The optimization gave no big difference in the beam performance for gun voltages in the range 450 - 500 kV. However, the voltage less than 425 kV essentially degrades the bunch length. Note, the rms bunch length should be kept 2 ps. Taking into account DC gun conditioning results, the value of 480 kV was decided for the following optimization.

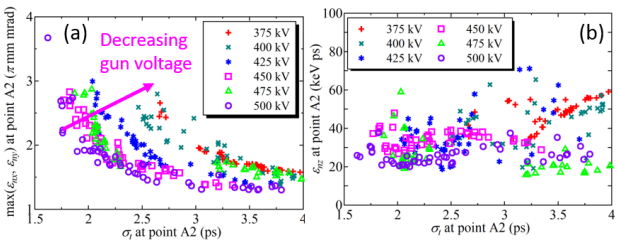

Figure 2: Gun voltage scan results at the exit of ML: (a) transverse emittance; (b) longitudinal emittance.

Effect of Initial Laser Temporal Distribution

Another task of the injector optimization was to investigate the influence of the initial laser temporal distribution. For the construction of the injector model for the previous operation a single Gaussian distribution was used. But in a common operation we are using a pulse stacking (one pulse is a stack of 7 Gaussian pulses with 40 ps FWHM). To reproduce a real laser time structure in the simulation, a 40 ps FWHM flat-top distribution, and a 40 ps FWHM flat distribution with 20% dip were introduced.

A comparison of the phase space distributions was done for all 3 options at the exit of ML. Since differences in results for the flat-top and the flat with 20% dip distribution were negligible, let us concentrate here on the comparison of the single Gaussian with flat. While Gaussian distribution has some particles near the beam core (Fig. 3 (a)), the phase space of the flat distribution looks smaller (Fig. 3 (b)). However, the transverse emittance is smaller for the Gaussian distribution. The reason is because the primary optimization was set up in the way to minimize the transverse emittance for the Gaussian laser pulse. The flat distribution has a shape closer to the real distribution. And the energy tail for it is reduced (comparing Fig. 3 (c) and (d)).Note that the curved shape of the energy distribution is again due to the optimization setup. Further studies showed the energy distribution to be flatter in the case when the longitudinal emittance is minimized.

Beam Parameters' Minimization

Now let us discuss the overall strategy of the injector optimization. Previously we have tried a simultaneous minimization of the bunch length and the transverse emittance [12].

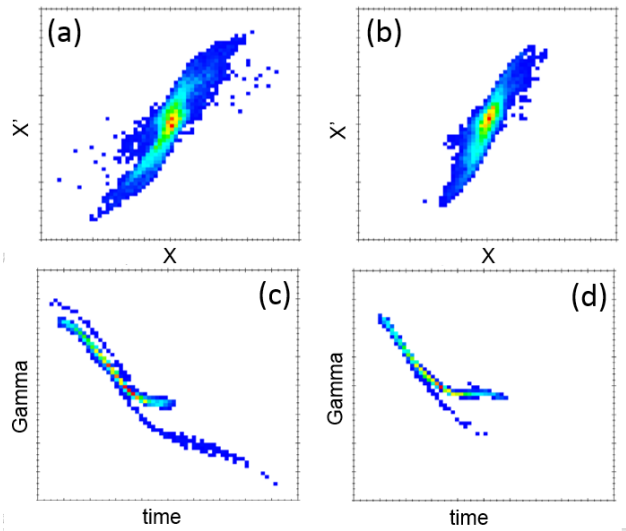

Figure 3: Comparison of the phase space at the exit of ML: XX' (a) and energy distribution (c) for single a Gaussian; XX' (b) and energy distribution (d) for a flat-top.

The result of this optimization was not satisfactory for FEL light production, since the bunch compression in the arc was not enough. Therefore, this time we have concentrated on the simultaneous minimization of the bunch length and the longitudinal emittance at the exit of the ML (Fig. 1). The constrains of the MOGA optimization are listed in Table 1. The first 2 conditions are dictated by the requirements for FEL light production. The last 2 conditions are for the optics matching. There are 13 optimization parameters of the MOGA. They include the current of the 1st solenoid (the current of the 2nd solenoid is typically zero), the buncher voltage, the injector cavities accelerating field, the 1st injector cavity phase offset, and straights of selected quadrupoles.

Table 1: Constrains of the MOGA Optimization

RMS bunch length	< 1.8 ps
Transverse rms emittance	< 2.4 π mm mrad
Betatron function	β_x < 8.0 m, β_y < 20.0 m
Hor. alpha function	-2.0 < α_x < 0.0
Vert. alpha function	-0.5 < α_y < 0.5

The result of a simultaneous minimization of the bunch length and the longitudinal emittance at the gun voltage of 480 kV is given at Fig. 4. The variety of 50 choices of injector settings are represented. One setting includes 3 values: the bunch length, the transverse emittance, and the longitudinal emittance. The marks are scattered at the figure to the left, while aligned along the curve at the figure to the right. This is again due to the optimization strategy to minimize simultaneously the bunch length and the longitudinal emittance. The setting marked with blue square with the 1.8 ps bunch length was chosen as a best candidate with all the values minimized.

ISBN: 978-3-95450-214-1 ISSN: 2673-5490 doi:10.18429/JACoW-IPAC2021-FRXB07

Now we have determined all the injector designed parameters for the following operation, i. e. the electron gun voltage is 480 kV, the injector energy is 5.1 MeV, the bunch charge is 60 pC, and the laser time structure is flat, FWHM 40 ps. What beam performance could be achieved at the exit of the ML? To summarize, the designed beam performance at the exit of the ML reads the transverse emittances are 1.74, 1.92 π mm mrad, the longitudinal emittance is 8.4 keV ps, the transverse beam sizes are 0.69, 0.35 mm, the bunch length is 1.8 ps, and the energy spread is 0.25%.

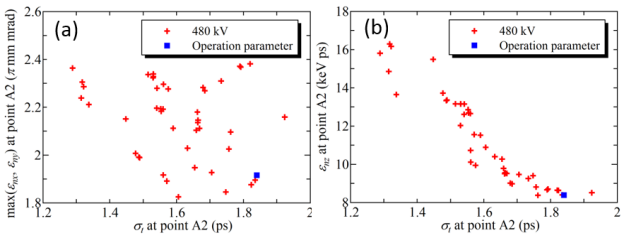

Figure 4: Optimization results at the ML exit: (a) transverse emittance; (b) longitudinal emittance.

COMPARISON WITH MEASUREMENT

When the injector is optimized properly, it is time to compare the designed performance with the measurements results that were obtained during the last run. Let us consider the buncher tuning result. To adjust a single particle motion without space charge effect, we operated the injector with 1 pC bunch charge. In order to adjust longitudinal dynamics, we measured energy response to the buncher phase. The beam energy was measured on the screen in the merger section (see Fig. 5 (a)). After fine accelerator voltage and phase tuning, the measured response was almost consistent with the design response (see Fig. 5 (b)).

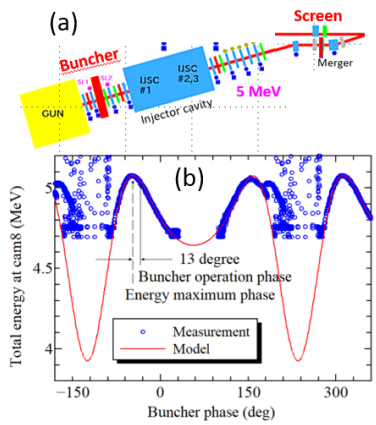

Figure 5: Buncher tuning: (a) injector layout; (b) buncher phase energy response.

Next topic to study is the optics matching with 60 pC. To adjust multi particle motion including space charge effect, we usually measure quadrupole-scan response. With our adjustment, the discrepancies became much smaller than the initial state. After quadrupole-scan responses corrected at each matching point we measured beam size at each screen in the injector line up to the exit of the ML (Fig. 1). Following Fig. 6, the measured beam sizes well agreed with the design beam sizes except for the exit of injector. The reason for the deviation of the vertical beam size at Cam3 still unclear. It is necessary to investigate the space charge effect including the time structure of the excitation laser. These issues are the next study topic. The last parameter to study is the emittance. The emittance was measured through the quadrupole-scan at the end of the ML. Thus, design values read ε_{nx} = 1.74 π mm mrad, ε_{ny} = 1.92 π mm mrad. While the measurement gave ε_{nx} = 2.87 ± 0.03 π mm mrad and ε_{ny} = 1.57 ± 0.02 π mm mrad. Easy to see that measured vertical emittances are in a good agreement with the design value. But the difference in horizontal emittances still remains since the real emittances may differ from design values.

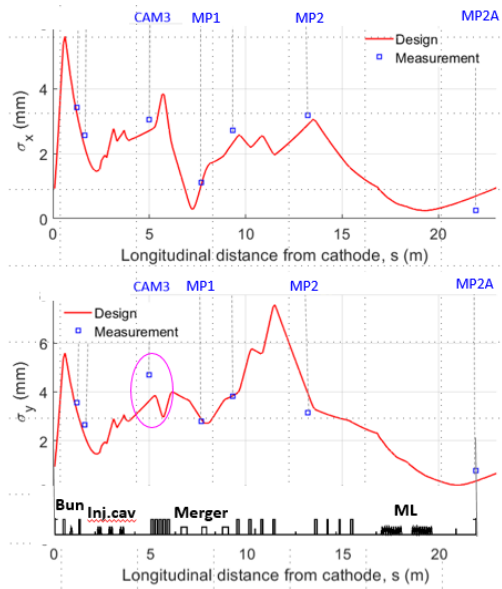

Figure 6: Designed and measured horizontal (top) and vertical (bottom) beam sizes after optics matching.

CONCLUSION

We achieved an appropriate beam performance at the undulator entrance (Fig. 1) by injector optimization with respect to: the electron gun voltage of 480 kV; the laser initial temporal distribution 40 ps FWHM flat-top; and the simultaneous minimization of bunch length and longitudinal emittance at the exit of the main linac. During the last run we produced IR-FEL light at the beam energy of 17.6 MeV [9]. Comparison of the designed performance and measured results demonstrated a good agreement in the transverse motion. However, the longitudinal motion needs additional investigations for bunch compression in the recirculation loop. To evaluate it is next study topic for the near future. Next big plan for the cERL operation includes, first, the CW operation with energy recovery, and second, the average beam current increase up to 10 mA.

ISBN: 978-3-95450-214-1 ISSN: 2673-5490 doi:10.18429/JACoW-IPAC2021-FRXB07

REFERENCES

[1] M. Akemoto *et al.*, "Construction and commissioning of the compact energy-recovery linac at KEK", *Nucl. Instrum. Meth. A*, vol. 877, pp. 197-219, 2018. doi:10.1016/j.nima.2017.08.051

[2] T. Miyajima *et al.*, "60 pC Bunch Charge Operation of the Compact ERL at KEK", in *Proc. 8th Int. Particle Accelerator Conf. (IPAC'17)*, Copenhagen, Denmark, May 2017, pp. 890-893. doi:10.18429/JACoW-IPAC2017-MOPVA019

[3] T. Hotei, R. Kato, and T. Miyajima, "Evaluation of 60pC Beam Performance at cERL Injector for ERL Based EUV-FEL", in *Proc. 29th Linear Accelerator Conf. (LINAC'18)*, Beijing, China, Sep. 2018, pp. 699–701. doi:10.18429/JACoW-LINAC2018-THPO009

[4] T. Obina *et al.*, "1 mA Stable Energy Recovery Beam Operation with Small Beam Emittance", in *Proc. 10th Int. Particle Accelerator Conf. (IPAC'19)*, Melbourne, Australia, May 2019, pp. 1482–1485. doi:10.18429/JACoW-IPAC2019-TUPGW036

[5] N. Nishimori *et al.*, "Operational experience of a 500 kV photoemission gun", *Phys. Rev. Accel. Beams*, vol. 22, no. 5, p. 053402. doi:10.1103/PhysRevAccelBeams.22.053402

[6] H. Sakai, "Industrial Applications of cERL", presented at ERL'19, Berlin, Germany, Sep. 2019, paper MOCOZBS02, unpublished.

[7] R. Kato *et al.*, "Development of mid-infrared free-electron laser based on cERL and its lasing experiment", presented at PASJ'20, online, Sep. 2020, paper THOT07, unpublished.

[8] K.Tsuchiya *et al.*, "Magnetic adjustment of the tandem undulators for the cERL-FEL", in *Proc. 17th Annual Meeting of Particle Accelerator Society of Japan (PASJ'20)*, online, Sep. 2020, pp. 850–852.

[9] R. Kato *et al.*, "Construction of an Infrared FEL at the Compact ERL", presented at the 12th Int. Particle Accelerator Conf. (IPAC'21), Campinas, Brazil, May 2021, paper TUPAB099.

[10] General Particle Tracer, http://www.pulsar.nl/gpt/.

[11] B. van der Geer and M. de Loos, "Multi-objective Genetic Optimization with the General Particle Tracer (GPT) Code", in *Proc. 6th Int. Particle Accelerator Conf. (IPAC'15)*, Richmond, VA, USA, May 2015, pp. 492-494. doi:10.18429/JACoW-IPAC2015-MOPJE076

[12] O. Tanaka *et al.*, "High bunch charge injector operation of cERL for infrared free electron laser test", in *Proc. 16th Annual Meeting of Particle Accelerator Society of Japan (PASJ'19)*, Kyoto, Japan, Jul.-Aug. 2019, pp. 1086–1090.